

COMPACT ASYMMETRIC COPLANAR STRIP-FED ANTENNA FOR WIDEBAND APPLICATIONS

D. Laila, V. Deepu, R. Sujith, C. K. Aanandan, K. Vasudevan, and P. Mohanan

Centre for Research in Electromagnetics and Antennas, Department of Electronics, Cochin University of Science and Technology, Cochin, Kerala, India; Corresponding author: drmohan@cusat.ac.in

Received 29 August 2008

ABSTRACT: An asymmetric coplanar strip-fed uniplanar antenna for wideband applications is presented. The resulting antenna offers a 2:1 VSWR bandwidth greater than 100% from 1.58 to 5.48 GHz covering the DCS/PCS/IEEE 802.11a/WiMAX bands. The antenna has an overall dimension of $44 \times 35 \text{ mm}^2$ when printed on a substrate of dielectric constant 4.4 and height 1.6 mm. The design equation is also presented in this article. The antenna exhibits good radiation characteristics and moderate gain in the entire operating band. © 2009 Wiley Periodicals, Inc. *Microwave Opt Technol Lett* 51: 1170–1172, 2009; Published online in Wiley InterScience (www.interscience.wiley.com). DOI 10.1002/mop.24287

Key words: asymmetric coplanar strip (ACS); uniplanar antenna; wideband antenna; DCS/PCS/IEEE 802.11a/WiMAX bands

1. INTRODUCTION

The demand for wideband antennas has experienced a booming growth in the wireless industry. Several interesting designs of wideband antennas have been demonstrated recently. A resonant aperture with stacked patches of different dielectric constants is employed for bandwidth enhancement in microstrip antenna [1]. The wideband E-shaped microstrip patch antenna in [2] incorporates two parallel slots in the patch to obtain a wide band. This antenna is excited by a probe feed and is mounted on large ground plane. The microstrip-fed planar Quasi-Yagi antenna presented in [3] has a bandwidth of 48%. These methods usually enlarge the volume and complexity of the antenna structure. Unlike the aforementioned microstrip configurations, uniplanar antennas are pop-

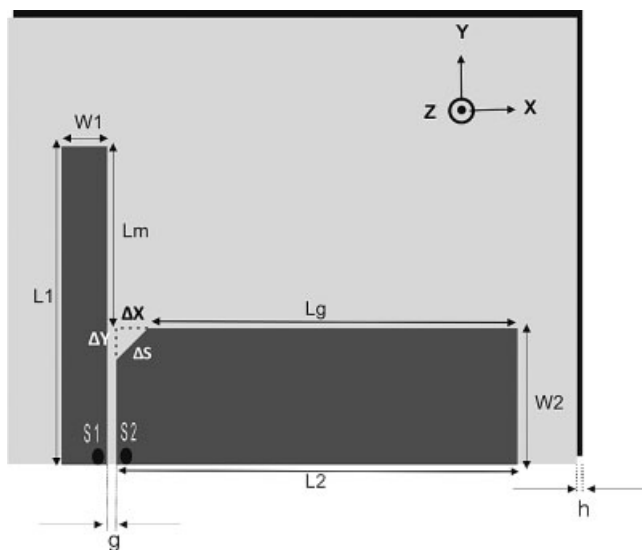


Figure 1 Antenna geometry ($L_2 = 44 \text{ mm}$, $W_2 = 15 \text{ mm}$, $L_1 = 35 \text{ mm}$, $W_1 = 5 \text{ mm}$, $g = 1 \text{ mm}$, $h = 1.6 \text{ mm}$, $\epsilon_r = 4.4$ and $L_v = L_m + \Delta y$, $L_h = L_g + \Delta x$, $\Delta x = \Delta y = 3.5 \text{ mm}$)

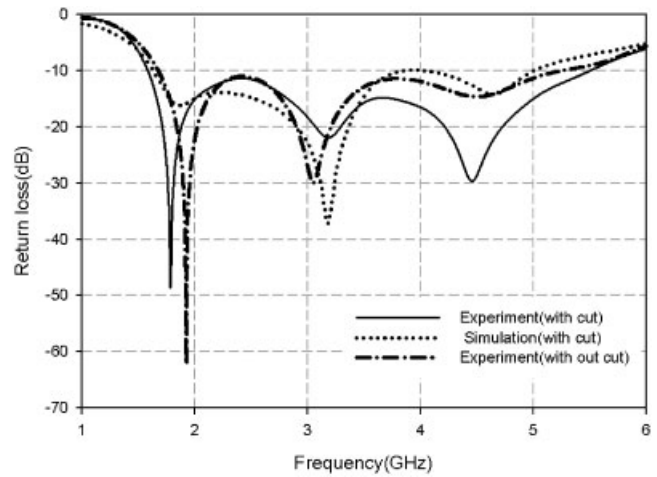


Figure 2 Experimental and simulated return loss characteristics of the proposed antenna

ular because of easy fabrication and integration with microwave monolithic integrated circuits (MMICs). Hwang [4] has reported a coplanar waveguide-fed T-shaped antenna with an overall dimension of $37.5 \times 80 \text{ mm}^2$ having 61.5% bandwidth. The asymmetric coplanar strip (ACS)-fed monopole antenna in [5] has only a bandwidth of 16%. In this article, we present a design of a simple and compact ACS-fed antenna for wideband applications. A very large bandwidth of 110% is obtained within an overall area of $35 \times 44 \text{ mm}^2$ on a substrate of dielectric constant 4.4 and thickness 1.6 mm.

2. ANTENNA GEOMETRY

Figure 1 shows the geometry of the proposed ACS-fed antenna. The antenna is designed on a substrate of dielectric constant 4.4 and height 1.6 mm. In a compact ACS feed, the lateral strip width (in this case W_1), the ground plane length (in this case L_2), and the gap g determine the characteristic impedance [6]. In this design, the strip dimensions are taken as $L_1 = 35 \text{ mm}$ and the width $W_1 = 5 \text{ mm}$. The ground plane dimensions are $L_2 = 44 \text{ mm}$, $W_2 = 15 \text{ mm}$ consists a gap g of 1 mm. The antenna is fed between the points S_1 and S_2 . These dimensions are chosen after exhaustive simulation and experimental studies for obtaining wide bandwidth.

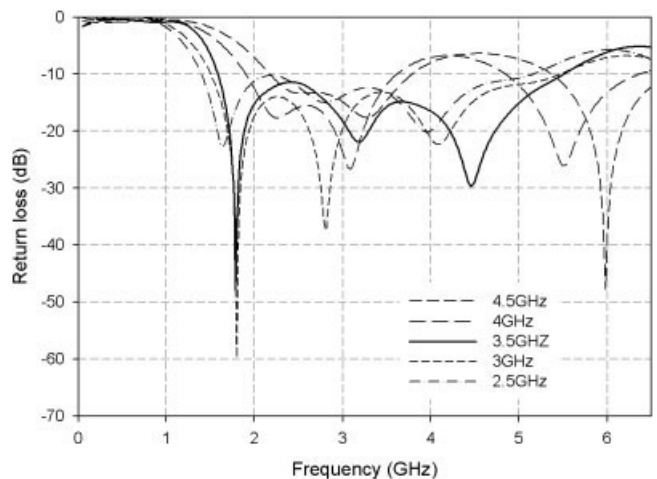


Figure 3 Return loss characteristics of the antennas with different center frequencies

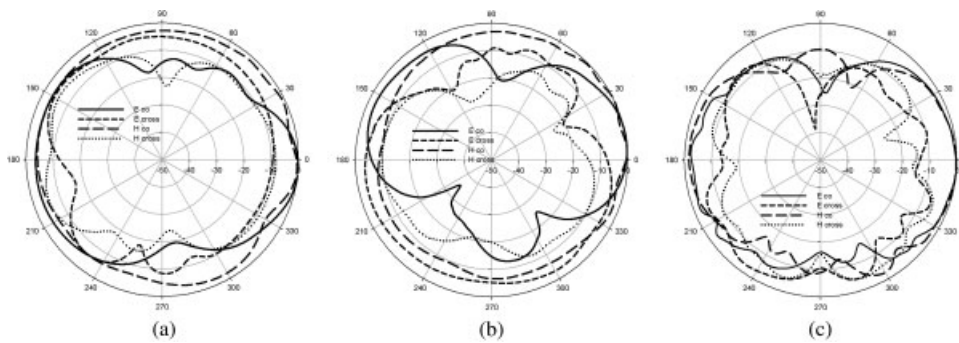


Figure 4 (a) Measured radiation pattern of the proposed wideband antenna at 1.85 GHz. (b) Measured radiation pattern of the proposed wideband antenna at 3.18 GHz. (c) Measured radiation pattern of the proposed wideband antenna at 4.4 GHz

The resulting antenna exhibits poor impedance matching. To improve the matching, a small triangular cut of dimensions $\Delta x \times \Delta y$ (shown in dotted lines) is inserted in the ground plane.

3. RESULTS AND DISCUSSION

The antenna is tested using HP8510C network analyzer. The Experimental and Ansoft HFSS simulated return loss curves of the antenna are shown in Figure 2. The return loss characteristics of the antenna without the triangular cut are also shown in the Figure 2 for comparison. It is found that this triangular cut is highly influencing the return loss characteristics of the antenna. The antenna exhibits a bandwidth of 110% from 1.58 to 5.48 GHz with good impedance matching. This wide bandwidth is due to the merging of three individual resonances centered at 1.85, 3.18, and 4.4 GHz. The broadband behavior of the antenna is confirmed by scaling the antenna for different frequencies and substrates.

3.1. Design Equation

To design a wideband antenna operating at a center frequency f_c , the dimensions L_v and L_h are taken as

$$L_h + L_v = 0.81 \lambda_c$$

$$L_h = 0.53 \lambda_c$$

$$L_v = 0.27 \lambda_c,$$

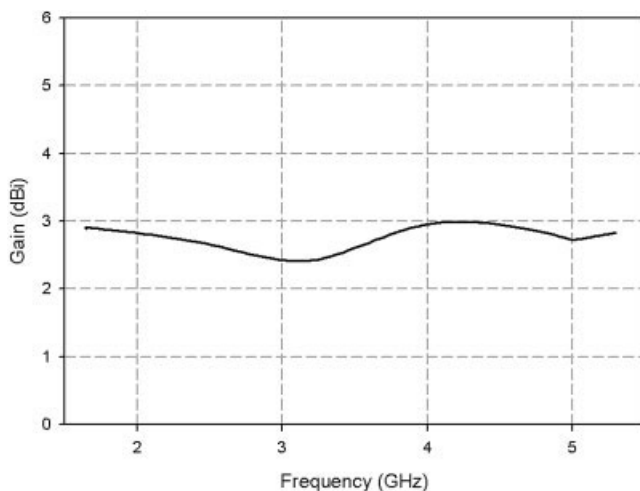


Figure 5 Measured gain of the proposed antenna

where λ_c is the free space wavelength corresponding to the center frequency f_c . It is also observed that the relation between vertical and horizontal lengths L_v and L_h as $L_h = 2 \times L_v$. To substantiate the veracity of the aforementioned equations, the dimensions are scaled and various prototypes for different frequencies are constructed and measured (see Fig. 3). It has to be noted that at higher frequencies, the bandwidth is found to be decreasing.

In the proposed antenna, the ground plane width W_2 is optimized as 0.33 times the length L_2 for maximum bandwidth. Similarly, the width W_1 is optimized as 0.2 times L_v when the gap g is 1 mm. From the series of simulation and experimental studies, it is found that the first resonance is due to the total length $L_v + L_h$, the second resonance is mainly due to L_h , and the third resonance is mainly due to L_v .

The principal E and H plane patterns of the antenna for the three resonances are shown in Figure 4. It has to be noted that the polarization of the antenna is tilted by -45° in the XY plane. This tilt is due to the asymmetry in the feed configuration. The antenna exhibits almost identical patterns with very good coverage.

The gain of the antenna is measured and depicted in Figure 5. The antenna exhibits a gain greater than 2.5 dBi in the entire band.

4. CONCLUSIONS

A simple, compact ACS-fed antenna operating from 1.58 to 5.48 GHz with 110% bandwidth is presented. This wideband antenna is obtained from exhaustive optimization studies on a simple ACS-fed strip monopole. The antenna exhibits good radiation characteristics with a gain better than 2.5 dBi in the entire operating band.

ACKNOWLEDGMENTS

The authors are grateful to UGC, Govt. of India, Kerala State Council for Science Technology and Environment (KSCSTE) and Defense Research Development Organization (DRDO), Govt. of India for providing financial assistance.

REFERENCES

1. S.D. Targonski and R.B. Waterhouse, Design of wide band aperture stacked patch microstrip antennas, *IEEE Trans Antennas Propag* 46 (1998), 1245–1251.
2. F. Yang, X.-X. Zhang, X. Ye, and Y. Rahmat-Samii, Wideband E shaped patch antennas for wireless communication, *IEEE Trans Antennas Propag* 49 (2001), 1094–1100.
3. N. Kaneda, W.R. Deal, Y. Qian, R. Waterhouse, and T. Itoh, A broad band planar Quasi-Yagi antenna, *IEEE Trans Antennas Propag* 50 (2002), 1158–1160.
4. R.B. Hwang, A broadband CPW-fed T-shaped antenna for wireless

communications, IEE Proc Microwaves Antenna Propag 151 (2004), 537–543.

5. V. Deepu, R.K. Raj, M. Joseph, M.N. Suma, and P. Mohanan, Compact asymmetric coplanar strip fed monopole antenna for multiband applications, IEEE Trans Antennas Propag 55 (2007), 2351–2357.
6. R. Garg, P. Bhartia, and I. Bahl, Microstrip antenna design hand book, 1st ed., Artech House, Boston, M.A, 2001, pp. 794–795.

© 2009 Wiley Periodicals, Inc.

DESIGN OF AN I-BAND LOW PHASE NOISE OSCILLATOR USING A NEW HAIR-PIN RESONATOR

Ki-Cheol Yoon,¹ Hyun-Wook Lee,¹ Jung-Geun Park,¹ Ki-Byoung Kim,² and Jong-Chul Lee¹

¹ Department of Wireless Communications Engineering, Kwangwoon University, 447-1 Wolgye-dong, Nowon-ku, Seoul 139-701, Korea; Corresponding author: jcllee@kw.ac.kr

² Samsung Thales Co. Ltd. San 14-1, Nongseo-Dong, Giheung-Gu Yongin City, Gyeonggi-Do, KOREA 446-712

Received 4 September 2008

ABSTRACT: In this article, a new high Q resonator is presented and it is applied to the design of an I-band oscillator. The measurement of the resonator itself shows that it provides a higher loaded quality factor when compared with the spiral-resonator. The oscillator is designed to be operated at 10 GHz using the new resonator to confirm the phase noise performance. The measurement results for the new hair-pin resonator oscillator show the output power of 8.18 dBm and the phase noise of -103.48 dBc/Hz at 100 kHz offset. © 2009 Wiley Periodicals, Inc. Microwave Opt Technol Lett 51: 1172–1174, 2009; Published online in Wiley InterScience (www.interscience.wiley.com). DOI 10.1002/mop.24283

Key words: spiral resonator; stepped impedance resonator (SIR); three stage level (TSL); quality factor; phase noise

1. INTRODUCTION

Generally, RF and microwave oscillators are implemented for frequency conversion and carrier generation, and widely used in all modern radar and wireless communication systems. It uses an active nonlinear device, such as a transistor and diode to convert the DC to a sinusoidal steady state RF signal [1, 2]. One example of the oscillator application is I-band or X-band down/up-converter in a microwave system. This I-band down or up-converter is implemented in a radar system, where it is transmitted in weapon control, navigation, piloting radar using the I-band satellite.

High- Q resonators are essential for low phase noise oscillators. Phase noise is one of the most important parameters in a communication system because it determines the overall performance of the system. The dielectric resonators are promising elements for these applications. However, they have a three-dimensional structure and their sizes are bulky. Therefore, they are limited to the on-chip integrated-circuit (IC) and MMIC (Monolithic Microwave Integrated Circuits) realization and are not adequate for mass production. In recent years, there have been numerous attempts to reduce the phase noise of the planar oscillators, which have some advantages for low cost and improved reliability [3]. Nevertheless, their phase-noise characteristics are inferior due to the poor Q factor of the planar resonator.

In this article, an I-band oscillator with low phase noise property using a new type of high- Q microstrip planar stop band resonator is presented. This circuit can be fabricated with HMIC

(Hybrid Microwave Integrated Circuits) or MMIC technique due to its entirely planar structure.

2. DESIGN OF THE HIGH-Q NOVEL RESONATOR

This article suggests a new microstrip resonator with high quality factor and an oscillator with low phase noise using this resonator. The design equation for generating the parameters of the equivalent three-stage level (TSL) structure is derived by new type of SIR (Stepped Impedance Resonator) model calculation. Also, the design of an I-band oscillator with low phase noise using this resonator is introduced.

The new type of SIR with TSL structure to be considered here is shown in Figure 1. The SIR is symmetrical and composed of three different characteristic impedances, Z_1 , Z_2 , and Z_3 [4, 5]. Here, Z_1 is the high impedance and Z_2 , Z_3 are the low impedances. For practical application, it is preferable to have equal electrical lengths. Then, the condition for the fundamental resonance of the TSL with SIR can be derived as,

$$\theta = \tan^{-1} \sqrt{\frac{K_i K_{i+1}}{K_i + K_{i+1} + 1}}, \quad \text{at } \theta_1 = \theta_2 = \theta_3 = \theta, Z_i \neq Z_{i+1} \quad (1)$$

where θ is electrical length for SIR unit and $K_i = Z_3/Z_2$ and $K_{i+1} = Z_2/Z_1$. The resonator's total electrical length at the fundamental resonance is given by,

$$\theta_T = 6\theta = 6 \tan^{-1} \sqrt{\frac{K_i K_{i+1}}{K_i + K_{i+1} + 1}} \quad (2)$$

The novel resonator using the equivalent circuit shown in Figure 1 and Eqs. (1) and (2) is shown in Figure 2. As shown in Figure 2, the value of Z_3 is made lower than Z_2 in order to control and improve the value of capacitance ($Z_2 > Z_3$). The main feature of this structure is to make resonance by connecting the Z_1 , Z_2 , and Z_3 with equal electromagnetic energy. The other method of increasing quality factor is decreasing the size of the gap between Z_2 and Z_3 , and the gap between the terminals (Z_3) through the tight coupling. Figure 3 shows the simulation and measurement results for the proposed resonator. From the figure, the simulated loaded quality factor is 222 and the measured external quality factor is better than 143 at the center frequency of 10.0 GHz and 10.08 GHz, respectively. To get a high Q resonator, the microstrip line widths at both end-parts are increased to decrease the characteristic impedance. These results can be compared with the simulated and measured loaded quality factors of 50 and 44, respectively, for the spiral resonator implemented for comparison in this research.

In fact, there are some differences in simulation and measurement results due to the loss in substrate with fabrication, the effect of load resistance, and cable loss included from the measurement

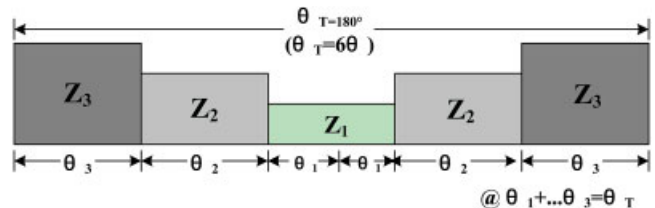


Figure 1 The equivalent model of a novel resonator with TSL structure in SIR. [Color figure can be viewed in the online issue, which is available at www.interscience.wiley.com]